Original Article

VEGF expression disparities in brainstem motor neurons of the SOD1^G93A ALS model: Correlations with neuronal vulnerability

Silvia Silva-Hucha [a,b,1], M. Estrella Fernández de Sevilla [a,1], Kirsty M. Humphreys [c], Fiona E. Benson [c], Jaime M. Franco [d], David Pozo [d,e], Angel M. Pastor [a,*], Sara Morcuende [a,*]

[a] Departamento de Fisiología, Facultad de Biología, Universidad de Sevilla, 41012 Seville, Spain
[b] Cell and Developmental Biology, University College London, Medawar Building, Gower Street, London WC1E 6BT, UK
[c] Division of Biomedical and Life Sciences, Faculty of Health and Medicine, Lancaster University, Lancaster LA1 4YQ, UK
[d] Andalusian Center of Molecular Biology and Regenerative Medicine-CABIMER, Junta de Andalucía-Universidad Pablo de Olavide-Universidad de Sevilla-CSIC, 41092, Seville, Spain
[e] Department of Medical Biochemistry, Molecular Biology and Immunology, Universidad de Sevilla Medical School, 41009 Seville, Spain

ABSTRACT

Amyotrophic lateral sclerosis (ALS) is a rare neuromuscular disease characterized by severe muscle weakness mainly due to degeneration and death of motor neurons. A peculiarity of the neurodegenerative processes is the variable susceptibility among distinct neuronal populations, exemplified by the contrasting resilience of motor neurons innervating the ocular motor system and the more vulnerable facial and hypoglossal motor neurons. The crucial role of vascular endothelial growth factor (VEGF) as a neuroprotective factor in the nervous system is well-established since a deficit of VEGF has been related to motoneuronal degeneration. In this study, we investigated the survival of ocular, facial, and hypoglossal motor neurons utilizing the murine SOD1^G93A ALS model at various stages of the disease. Our primary objective was to determine whether the survival of the different brainstem motor neurons was linked to disparate VEGF expression levels in resilient and susceptible motor neurons throughout neurodegeneration. Our findings revealed a selective loss of motor neurons exclusively within the vulnerable nuclei. Furthermore, a significantly higher level of VEGF was detected in the more resistant motor neurons, the extraocular ones. We also examined whether TDP-43 dynamics in the brainstem motor neuron of SOD mice was altered. Our data suggests that the increased VEGF levels observed in extraocular motor neurons may potentially underlie their resistance during the neurodegenerative processes in ALS in a TDP-43-independent manner. Our work might help to better understand the underlying mechanisms of selective vulnerability of motor neurons in ALS.

Introduction

Amyotrophic Lateral Sclerosis (ALS) is a neurodegenerative disease affecting motor neurons responsible for controlling voluntary muscles in the spinal cord, brainstem, and cortex [1]. This disease causes the patient's death in approximately 2–5 years following the onset of symptoms, usually due to respiratory failure, and affects 1–2 people out of every 100,000. In ALS, both brain (upper) motor neurons and brainstem and spinal cord (lower) motor neurons progressively degenerate or die, thus ceasing to send information to the muscles, triggering progressive atrophy of the skeletal musculature [2]. Excessive fatigue, fasciculations

(contractions of the muscle), dysarthria (difficulty speaking), dysphagia (inability to swallow), and dyspnoea (respiratory problems) are observed. Finally, the central nervous system loses the ability to initiate and control the movement of the muscles [2].

Roughly 90–95% of ALS cases are sporadic, with only 5–10% of patients having a genetic family history assessment [1]. Currently, several genes are linked to familial ALS [3–5]. Approximately 15–20% of the familial cases can be attributed to mutations in the gene responsible for encoding antioxidant copper/zinc superoxide dismutase (SOD1), located on chromosome 21 [3,5]. Frequently, familial cases associated with alterations in the SOD1 gene follow an autosomal dominant inheritance

pattern. A wide variety of likely pathogenic mechanisms including oxidative stress, excitotoxicity, inflammation, mitochondrial and neurofilament dysfunction, protein aggregation, abnormalities in axonal transport, and RNA metabolism has been identified to primarily affect motor neurons although other cell types are clearly implicated [4]. One of the most widely used and well-characterized animal models of ALS is the transgenic mouse expressing the SOD1[G93A] protein, that harbors a human mutation consistent in a replacement of Gly by Ala in position 93 (referred to as SOD mice from now on). This murine model shows a phenotype similar to the human form of ALS [3–5]. Motor impairments appear around the 60th day, characterized by a gradual onset of clinical weakness that ultimately leads to paralysis and culminates in mortality by the 140th day [6–8].

Remarkably, a distinctive feature of neurodegenerative processes observed in both SOD mice and ALS patients, is the presence of specific neuronal populations that exhibit heightened resistance to degeneration when contrasted with other motor groups that succumb to degeneration earlier. This phenomenon underscores the varying susceptibility of distinct neuronal populations to degeneration, with certain populations demonstrating extended survival times for reasons that remain presently unidentified [7,9–11]. In particular, motor neurons within the oculomotor system, responsible for eye movements and situated in the brainstem, as well as motor neurons located in Onuf's nucleus within the sacral spinal cord, which govern pelvic muscle function, exhibit a reduced susceptibility to degeneration. These specific neuronal populations remain unaffected in cases of human ALS and in SOD mice models, in stark contrast to other motor systems, such as the facial and hypoglossal systems [6,12]. Indeed, it has been conclusively demonstrated that individuals with ALS, even in the late stages of the disease, retain the capacity for ocular movement, whereas other motor systems degenerate significantly earlier [13,14].

There is evidence supporting the notion that increased expression of certain trophic factors, such as vascular endothelial growth factor (VEGF), may play a role in enhancing resistance to neurodegenerative diseases, including ALS [15–17]. In this context, genetically engineered mice with a deletion in the hypoxia response element within the promoter region of VEGF (referred to as VEGF[δ/δ] mice) [18] exhibited an inability to increase VEGF levels in response to hypoxic conditions, resulting in motor neuron degeneration and premature mortality, presenting symptoms remarkably similar to those observed in ALS disease. This suggests that reduced VEGF levels could play an essential role in the mechanisms underlying motor neuron degeneration. Subsequent studies have further confirmed the downregulation of VEGF in the spinal cord of SOD mice [16,19]. Consistent with this observation, reports indicate a reduction in VEGF levels in both the spinal cord and cerebrospinal fluid (CSF) of ALS patients [20–22].

To date, while extensive research has been done in spinal motor neurons of ALS patients and preclinical models [16,18,23–29], data are scarce in brainstem motor nuclei [30,31], where important differences in survival are observed (for review, see Refs. [32,33]). Recently, we reported an increased level of VEGF in rat motor neurons of the oculomotor nuclei than other brainstem nuclei, such as the facial and hypoglossal [34,35], which could contribute to their heightened resistance to neurodegeneration following injury or in degenerative diseases like ALS. Consequently, it becomes of high relevance to investigate whether VEGF is associated with the enhanced survival of extraocular motor neurons in SOD mice in comparison to non-ocular motor neurons. Such research provides a framework to investigate the differential vulnerabilities observed during the progression of ALS disease.

A common feature observed in the late stages of human ALS is the presence of cytoplasmic protein aggregates, primarily composed of a nuclear protein known as TAR DNA-binding protein 43 (TDP-43, Transactive response DNA-binding protein 43 kDa) which could be related to clearing of nuclear TDP-43 [4,36–40]. TDP-43 has been identified as translocating from the nucleus to the cytoplasm and forming aggregates, a phenomenon shared between ALS and certain forms of

frontotemporal lobar degeneration (FTLD) [41]. This aberrant localization of TDP-43 has been proposed as a distinctive hallmark of human ALS pathology [36,42]. Even though the presence of TDP-43 aggregates in the SOD1 animal model for ALS is still a matter of debate [43,44], a number of studied have characterize abnormal TDP-43 alterations [45–47]. Consistent with a TDP-43/SOD1 link, a recent study has revealed a protein kinase co-localising with TDP-43 cytoplasmic aggregates in a cell model [48] which is dysregulated in SOD1 mouse spinal cord [49]. However, this phenomenon has not been explored in the brainstem motor nuclei of SOD mice. Noteworthy, the administration of VEGF has been demonstrated to reduce TDP-43 aggregates in the motoneuronal cell line NSC-34 when exposed to ALS-CSF [50].

Thus, the central hypothesis of this study proposes that the heightened resistance observed in motor neurons within the oculomotor system against neurodegeneration may be attributed to an increased expression of VEGF. Consequently, we considered it relevant to investigate and compare the distribution patterns of VEGF between oculomotor neurons and other brainstem motor neurons that exhibit greater susceptibility to neurodegeneration, such as the facial and hypoglossal motor neurons, using the SOD mouse model of ALS at various stages of the disease. Therefore, we have also undertaken the study of the subcellular localization of TDP-43 in motor neurons of both the oculomotor and non-oculomotor nuclei within the brainstem, aiming to discern if potential variations in VEGF levels between vulnerable and resistant motor neurons are accompanied by differences in the occurrence of mislocalization of TDP-43 at advanced degeneration stages in this murine model.

Methods

Animal model

Transgenic males B6SJL-TgN(SOD1-G93A) 1Gur/J (Jackson Laboratory, No. 002726), carrying the human SOD1 gene with the G93A point mutation (mSOD1) [7] were purchased from Jackson Laboratory (USA). To establish and maintain a colony at the rodent facility of the CABIMER institute, wild-type B6SJLF1/J females were purchased from Jackson Laboratory (USA) and used to breed with male transgenic for the mSOD1 gene. At weaning time, littermates were identified through ear punching and separated into different cages according to gender. Thus, WT stands for non-transgenic mice, while SOD stands for transgenic mice carrying the human G93A SOD1 mutation. Genomic DNA was extracted from mice tail snips by phenol-chloroform method to run a qPCR procedure for genotyping and verifying a high copy number of the hSOD1 transgene in the progeny. The specific primers used for hSOD1 transgene amplification were: forward primer, 5′-CAT CAG CCC TAA TCC ATC TGA-3'; reverse primer, 5′-CGC GAC TAA CAA TCA AAG TGA-3′. Internal control IL-2 gene primers were: forward primer, 5′-CTA GGC CAC AGA ATT GAA AGA TCT-3'; reverse 5′-GTA GGT GGA AAT TCT AGC ATC ATC C-3′). Genomic DNA from SOD1[G93A]-positive mice was quantified in a NanoDrop equipment, adjusted to 4 ng/μl, and a SensiFAST SYBR Lo-ROX kit was used for amplification. The thermal profile consisted of an initial denaturation step at 95 °C for 10sec, followed by 40 cycles of 95 °C for 15sec, 60 °C for 35sec, 72 °C for 32sec and finally, a dissociation cycle, to verify that only one product was amplified. The Applied Biosystems S7500 FAST Real-Time PCR was used. For rotarod performance tests, mice received three training sessions before the experiments to learn how to stand and walk on the rotating rod (Ugo Basile, Varese, Italy). For testing, each session consisted of three trials with a maximum duration of 5 min each and 15 min of resting between trials (Fig. S1-a). Performance was measured in ramping sessions from 4 to 16 rpm within 270 s and a cut-off time of 300 s. Performance was quantified as latency time, the time the animals remained walking on the rotarod before falling down or cut-off time. For each session, the best latency time was recorded. The body weight of animals was measured weekly (Fig. S1–b). Kaplan-Meier curve of the colony is represented in Fig. S1–c. All animals were housed in 4–8 animals/cage, at standard conditions of 25 °C ambient

temperature, under 12 h light/12 h dark cycle, and receiving food and water *ad libitum*.

Male mice (n = 32, WT and SOD 8 and 12 weeks: 5 mice/group), WT and SOD 16 weeks: 6 mice/group) were distributed in different groups as follows. Three groups of animals of different ages were selected to represent different stages of the degenerative process according to previous studies [6,8,10,12]: 8-weeks-old, corresponding to the onset and appearance of symptoms, 12-weeks-old, where symptoms are evident and the disease progresses, and 16-weeks-old, corresponding to an advanced stage of the disease. Another three groups of age-matched wild-type (WT) littermates from the same colony were used as controls. All experimental procedures were performed under the guidelines of the European Union (2010/63/EU) and the Spanish legislation (RD. 53/2013, BOE 34/11370-421) for the use and care of laboratory animals and approved by the local committees for animal research CEEA-CABIMER-25-2010 and CEEA-US2015-15/3.

Animals were anaesthetized using sodium pentobarbital (50 mg/kg, i.p.), and perfused using a peristaltic pump with 10 ml of physiological saline, followed by 25 ml of 4% paraformaldehyde in 0.1 M sodium phosphate buffer, pH 7.4. Brainstems were removed and immersed in a solution of 30% sucrose in sodium phosphate-buffered saline (PBS) until sinking. Tissue was then cut into 40 μm-thick coronal sections using a cryostat (Leica CM1850, Wetzlar, Germany), and slices were collected in six parallel series in PBS-glycerol (1:1). Series 1 and 4 of each animal were used for stereology, and at least one series was used for every immunohistochemical experiment.

Western Blot with TDP-43 antibody in mouse brain

Firstly, to verify the specificity of the antibody against the TDP-43 protein in mice, the presence of the protein was studied employing the Western Blot technique in the brain tissue of control mice. Adult WT mice (n = 3) were anaesthetized, and brains were removed and incubated in a lysis buffer containing a cocktail of protease and phosphatase inhibitors (Roche Diagnostics GmbH, Germany, 11836170001) for 20 min on ice. The homogenate was centrifuged at 13,000 rpm for 30 min at 4 °C. The supernatant was collected, and proteins were quantified by the Bradford method. Twenty-five μg of total protein were mixed 1:1 with the loading buffer (0.0625 M Tris-HCl pH 6.8, 10% Glycerol, 2% SDS, 5% β-mercaptoethanol and 0.05% Bromophenol Blue) [35]. Before electrophoresis, proteins were denatured in a 90 °C bath for 6 min.

Electrophoresis was performed in a 15% acrylamide SDS PAGE at a constant voltage of 100 mV for 90 min. Then, proteins were transferred to a previously activated PVDF membrane (Bio-Rad, CA, USA, 1620177) at 80 mV for 40 min in a transfer buffer composed of Trizma-base, Glycine and 0.16% SDS. Membranes were then blocked with Tris-buffered saline with 0.1% Tween (TBS-Tween) and 5% bovine serum albumin for 1 h and then incubated with the primary anti-TDP-43 antibody at 4 °C overnight under stirring. The antibody used was DB9 (mouse anti-TDP-43 IgG, 1:1000, Millipore, CA, USA, MABN774), a mouse monoclonal antibody raised against recombinant His-tagged human TDP-43 residues 208–414 expressed in *Escherichia coli* and purified by Immobilised Metal Affinity Chromatography and SDS-PAGE. The antibody has specificity for a short nine amino acid epitope (GAFSINPAM) conserved at residues 314–322 in humans and mice (Fig. S2). After washing three times in TBS-Tween, membranes were incubated with the secondary antibody (goat anti-mouse IgG coupled to horseradish peroxidase (HRP), 1:10,000, Jackson ImmunoResearch, PA, USA, 115-035-003) for 1 h at room temperature (RT). The signal was developed with the Western Blot development kit (WesternBright Quantum K-12042-D20), and bands were visualized with a chemiluminescence system (Vilber, Fusion - Solo S) and the Evolution Capture software. The membranes were then washed with Stripping Buffer and re-incubated with a primary antibody against glyceraldehyde-3-phosphate dehydrogenase (GAPDH), a protein used as load control (mouse anti-GAPDH IgG, 1:1,000, Millipore, MAB374), and subsequently with an HRP-coupled secondary antibody (goat anti-mouse IgG coupled to HRP, 1:10,000, Jackson ImmunoResearch, 115-035-003).

Stereology procedures

One out of three serial sections were mounted on homemade gelatinized slides and stained by immersion in the 0.5% Toluidine Blue dye in 0.1 M acetate buffer pH 4.2 for 4 min. After rinsing, they were dehydrated by passing through increasing concentrations of ethanol (70%, 96%, and 100%). Slices were then submerged for 5 min in xylol, covered using the mounting medium DPX, and allowed to dry.

The total number of neurons (N) in the different brainstem nuclei was estimated following the Cavalieri principle [51,52], where calculations are done indirectly by nucleus volume. To obtain stereological images, we used the New Cast program (Visiopharm, Denmark), which monitors and randomizes the counting, and an Olympus BX61 optical microscope. Firstly, a superimage was taken with all sections, and then ROIs (regions of interest) corresponding to the brainstem nuclei of the study were delimited. Secondly, a template of Cavalieri points (Cv) was cast at 10x magnification, and the Cv points within the delimited nuclei were quantified. In the formula of total nucleus volume (VN): ΣP is the sum of the Cavalieri points of a nucleus, A(p) is the area associated with the point, and T corresponds to the distance between the sections, which is calculated by multiplying the thickness of the cut by three since one out of three sections were analyzed.

Total core volume (VN) = ΣP × A(p) × T

Cell counting was performed at 20x magnification using randomly distributed dissectors. This tool, also known as the counting box, is a virtual frame unbiasedly generated across our chosen ROIs, where to perform the cell counting. In the dissector volume (VD) formula: ΣD is the sum of the dissectors in a nucleus, and A(d) is the area associated with the dissector.

Dissector volume (VD) = ΣD × A(d) × thickness of the cut

Lastly, after quantifying all neurons (N) in optical dissectors, we calculated the total number of cells with the VN and VD calculated before.

Number of total neurons = N × VN / VD

Immunohistochemistry

Double immunohistochemistry against VEGF and ChAT

Parallel sections from the same animals described above were immersed in a blocking solution with 0.1% Triton X-100 in PBS (PBS-T) and 10% normal donkey serum (NDS, Sigma Aldrich, Saint Louis, MO, USA) for 45 min. Subsequently, sections were incubated overnight at RT and shaking in the primary antibody against VEGF (rabbit anti-VEGF A-20 IgG, 1:50, Santa Cruz Biotechnology, CA, USA, SC-152) diluted in PBS-T + 5% NDS + 0.1% sodium azide (Az-Na). After washing with PBS-T, sections were incubated in the dark with the secondary antibody coupled to the fluorophore fluorescein-5-isothiocyanate (FITC) (donkey anti-rabbit IgG FITC, 1:50, Jackson ImmunoResearch, 711-095-152) for 2 h in shaking at RT. Next, for identifying motor neurons, sections were incubated in a solution with the primary antibody against choline-acetyl-transferase (ChAT), used as a marker for motor neurons (goat anti-ChAT IgG, 1:500, Millipore, AB144P) overnight at RT. Then, sections were washed and incubated in a secondary antibody coupled to the fluorophore tetramethyl-rhodamine 5,6-isothiocyanate (TRITC) (donkey anti-goat IgG TRITC, 1:50, Jackson ImmunoResearch, 705-025-003) shaking for 2 h at RT and darkness. After washing, the serial sections were mounted on gelatinized slides and covered with a mounting medium for immunofluorescence (Sigma F4680).

Double immunohistochemistry against TDP-43 and ChAT

Another set of parallel brainstem sections from the same animals was incubated in boiling 10 mM citrate buffer, pH 6, for 10 min for antigen retrieval. Then, sections were washed twice in PBS-T and blocked with NDS 10% for 45 min. Sections were incubated with DB9 anti-TDP-43 Mab (mouse anti-TDP-43 IgG, 1:500, Millipore, MABN774) in a solution of 0.1% PBS-T-Az-Na 5% NDS 5% overnight at RT. Afterward, sections were incubated in the dark with a secondary anti-mouse antibody coupled to TRITC (donkey anti-mouse IgM TRITC, 1:100, Jackson Immuno Research 715-025-020) for 2 h at RT. After washing, for the identification of motor neurons, sections were incubated overnight in a solution with the primary antibody against ChAT, as mentioned above, followed by incubation in a secondary anti-goat antibody coupled to FITC (donkey anti-goat IgG FITC, 1:100, Jackson Immuno Research, 705-095-003) for 2 h at RT. Sections were mounted in gelatinized slides and covered.

Confocal microscopy analysis

The immunofluorescent staining was visualized with a Zeiss LSM 7 DUO scanning confocal microscope (Carl Zeiss, Jena, Germany), equipped with an argon laser for visualization of FITC-labelled cells (green, excitation wavelength 488 nm), and a DPSS laser for TRITC (red, excitation wavelength 543 nm). The images were captured sequentially using a Plan-Apochromat 40X Oil DIC M27 objective, numerical aperture 1.3, pixel size/sampling size 4.8, and were processed and archived by the Zen Software Light Edition Software (Carl Zeiss, Jena, Germany). Analysis of the images taken with the confocal microscope was carried out using ImageJ software (NIH, USA).

For VEGF immunostaining analysis, the somata of motor neurons, except for the nucleus, was outlined in the red channel (ChAT), and measurements of the optical density of the green channel (VEGF) were performed in the selected area to quantify VEGF levels in motor neurons. For background correction, five background samples of a size comparable to a motor neuron were analyzed in areas devoid of motor neurons in every image, and the average of the values obtained was considered as the background level. The optical density of each analyzed cell was divided by the background level in each corresponding image [9,34]. For TDP-43 analysis, the nucleus was outlined in the image in the red channel (TDP-43), and its area was compared with that of the cytoplasm of motor neurons labelled in green (ChAT) to check if there was mislocalization of TDP-43 from the nucleus to the cytoplasm, and TDP-43 optical density was also measured in the nucleus of identified motor neurons.

Statistical analysis

For the stereological data, to detect differences in the survival of the motor neurons between the different time points, a One-way analysis of variance (ANOVA) was carried out, followed by the *post hoc* Holm-Sidak method for all pairwise multiple using SigmaPlot 11 (Systat Software, Inc., Chicago, IL, USA). In addition, a Two-way-ANOVA test was done to see differences in the number of surviving neurons between the different nuclei (factor 1) and the different genotypes (factor 2) in every survival stage. Data were expressed as mean ± standard error of the mean, and the level of significance taken was $p < 0.05$.

For VEGF, the data obtained were subjected to One-way- and Two-way-ANOVA tests to detect differences in the expression of VEGF in the different nuclei (factor 1) and the different stages (factor 2). Comparisons between phenotypes were also performed. The One-way-ANOVA test was also employed to compare the optical density of TDP-43 across nuclei. The data were expressed as mean ± standard error of the mean. The level of significance taken was $p < 0.05$. The statistics were performed in the SigmaPlot 11 program.

Results

In this study, we assessed the survival rates of brainstem motor neurons in both control and SOD mice throughout the progression of the degenerative process. Furthermore, we characterized the presence of VEGF and TDP-43 in the oculomotor nuclei and compared it with other non-oculomotor brainstem motor nuclei, such as the facial and hypoglossal nuclei. To achieve this, we employed stereological techniques for neuron quantification, and conducted double fluorescent immunohistochemistry to detect the presence of VEGF, TDP-43 and ChAT within the motor neurons of the examined nuclei.

Survival of brainstem motor neurons in SOD mice

The total number of motor neurons present in each brainstem nucleus was determined by stereological methods at different survival stages (8, 12 or 16 weeks) in both control and SOD animals. Nissl staining was employed to allow locating the motor nuclei within the mouse brainstem and to identify the respective motor neurons.

In WT animals, no reduction in the motor neuron count was observed in any brainstem motor nuclei examined (abducens, trochlear, oculomotor, facial and hypoglossal nuclei) associated with increasing age. Fig. 1 displays photomicrographs of Nissl staining corresponding to the oculomotor (representative for ocular motor nuclei), facial and hypoglossal nuclei. The abducens and trochlear nuclei are shown in Fig. S3. Therefore, no significant differences were detected in the total cell number quantified at 8, 12, or 16 weeks of age (Table 1) across any of the nuclei in WT mice (Fig. 2).

However, the stereological study of motoneuronal survival in SOD mice unveiled a significant decrease in the count of facial (*$p < 0.05$; $F_{(2,7)}$: 9.22; One-way–ANOVA test; factor: time) and hypoglossal (*$p < 0.05$; $F_{(2,8)}$: 5.03; One-way–ANOVA test; factor: time) motor neurons in SOD mice over the course of their survival (Figs. 1 and 2). In contrast, no decrease in the motor neuron count was observed in any of the extraocular motor nuclei of the SOD model mice (Table 1).

As can be observed, the facial and hypoglossal nuclei exhibited the most pronounced neuronal loss when comparing images (Fig. 1; i *vs* l; o *vs* r) and numerical data (Table 1 and Fig. 2) between control and SOD animals at 16 weeks. However, no neuronal loss was detected in the abducens, trochlear and oculomotor nuclei (Fig. 2).

The results of the statistical analysis conducted at each of the survival stages yielded the following outcomes. At 8 weeks of survival, there were no statistically significant differences in the number of motor neurons located within both the extraocular nuclei or non-extraocular nuclei when comparing WT and SOD mice. However, at 12 and 16 weeks, a significant decline in motor neurons was evident in the facial and hypoglossal nuclei of SOD mice compared to their age-matched littermate controls (#$p < 0.05$; ##$p < 0.01$; 12 weeks $F_{(1,28)}$: 23.99; 16 weeks $F_{(1,31)}$:14.66); Two-way–ANOVA test; factors: genotype and nuclei). Specifically, at 12 weeks, the number of motor neurons in the facial nucleus was approximately 26% lower in SOD animals than in WT animals, and this reduction was sustained at 16 weeks of survival. In the hypoglossal nuclei, the loss of motor neurons was roughly 20% at 12 weeks and increased severely to 40% in the final stage (Table 1 and Fig. 2).

For the oculomotor nuclei, no significant differences were observed between control and transgenic mice during these advanced stages. Consequently, the numbers of neurons within these nuclei remained stable, confirming the survival of these motor neurons throughout disease progression (Table 1 and Fig. 2).

In summary, these findings indicated the absence of neuronal loss in the extraocular motor neurons over the course of the disease development. On the contrary, in the facial and hypoglossal nuclei of SOD mice, neuronal loss was observed throughout progression of the symptoms (12 weeks) and continued until the end-point of the experiment (16 weeks).
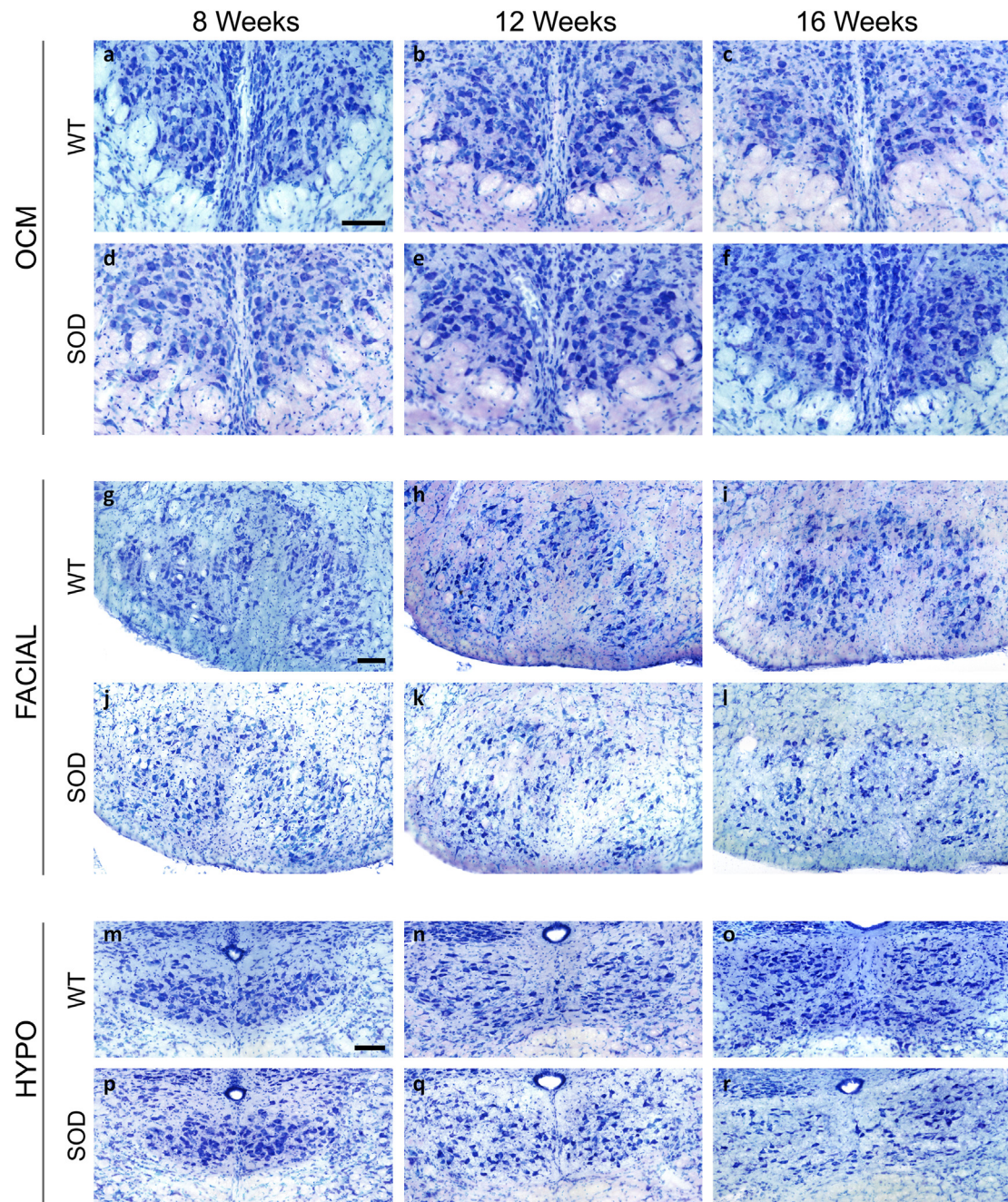
Fig. 1. Nissl-stained motor neurons in brainstem nuclei in SOD mice. Representative Nissl-stained sections of brainstem nuclei from WT and SOD mice in different stages of ALS disease, showing motor neurons in oculomotor (OCM; a-f), facial (g–l) and hypoglossal (HYPO; m-r) nuclei. Note the substantial reduction in the number of motor neurons at 16 weeks in facial (l) and hypoglossal (r) nuclei of SOD mice compared to their WT littermates (i and o, respectively). Calibration bars: 100 µm.

Table 1
Brainstem motor neuron survival.

Nucleus	8 weeks		12 weeks		16 weeks	
	WT	SOD	WT	SOD	WT	SOD
ABD	702.28 ± 75.99	726.64 ± 51.76	674.37 ± 78.58	547.41 ± 28.21	626.33 ± 54.54	534.60 ± 56.57
TROC	694.09 ± 123.38	567.98 ± 68.98	652.73 ± 54.39	535.31 ± 12.60	555.36 ± 26.21	522.60 ± 81.27
OCM	825.57 ± 27.69	797.73 ± 71.05	840.26 ± 94.80	991.31 ± 206.68	1115.59 ± 76.70	1083.89 ± 105.71
FACIAL	6520.16 ± 268.96	6316.64 ± 208.42	7347.98 ± 245.82	5436.24 ± 248.86	6492.95 ± 428.05	4830.34 ± 314.00
HYPO	2782.85 ± 128.89	2330.10 ± 158.70	2347.10 ± 175.21	1868.40 ± 268.11	2614.57 ± 184.86	1568.94 ± 128.68

Stereological quantification of the number of motor neurons in the brainstem nuclei of WT and SOD mice at the different stages of survival. ABD: abducens; TROC: trochlear; OCM: oculomotor. Data are expressed as mean ± standard error of the mean.
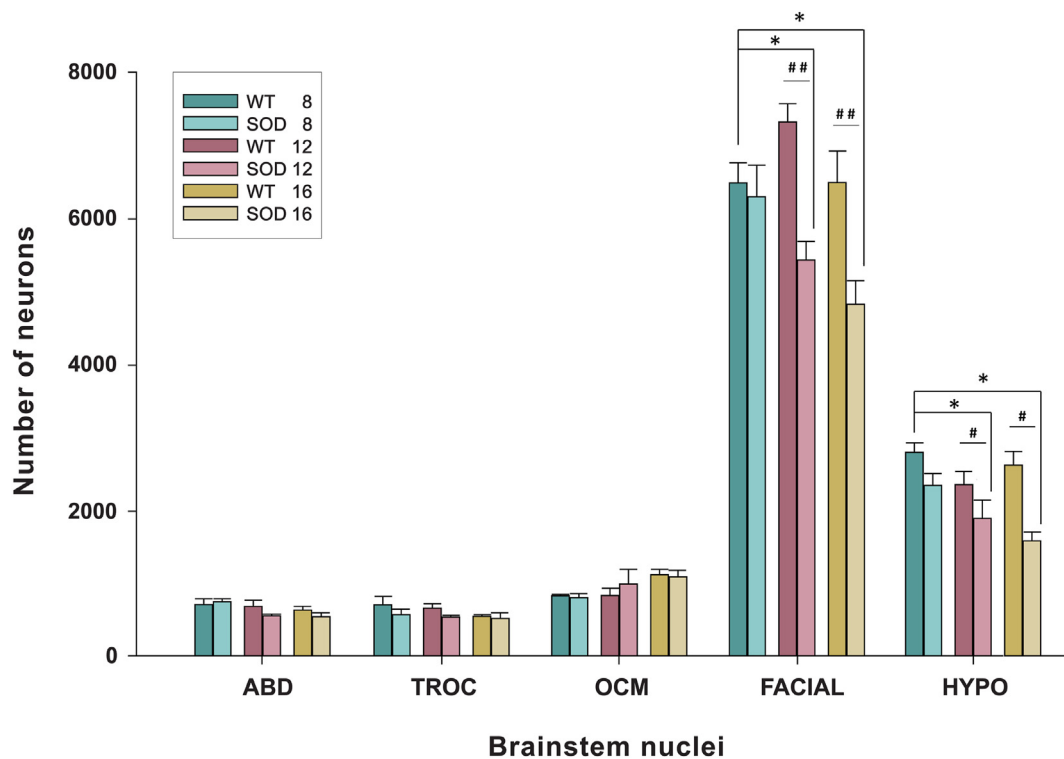
Fig. 2. Higher survival of extraocular motor neurons in SOD mice. The stereological study of motoneuronal survival revealed a significant reduction in the number of facial and hypoglossal (HYPO) motor neurons throughout the development of the disease in SOD mice (*; $p < 0.05$; One-way-ANOVA test; factor: survival time; significant differences to WT 8-weeks-survival). On the other hand, no reduction was observed in the extraocular motor nuclei (ABD: abducens; TROC: trochlear; OCM: oculomotor). Comparisons at each of the survival stages rendered a significant neuron loss in the facial and hypoglossal nuclei of SOD mice compared with the WT mice at 12 and 16 weeks of survival (#$p < 0.05$; ##$p < 0.01$; Two-way–ANOVA test; factors: genotype and nuclei).

Expression of VEGF in motor neurons of the brainstem at different stages of survival

We aimed to study the presence of the VEGF protein within the motor neurons of the abducens, trochlear and oculomotor nuclei, comparing it with the VEGF expression in the facial and hypoglossal nuclei. These experiments were conducted using WT and SOD mice aged 8, 12 and 16 weeks. For this purpose, double immunofluorescent staining was carried out against VEGF and ChAT, and the VEGF immuno-positive signals across the different motoneuronal pools were compared between WT and SOD mice at different stages of survival.

Immunoreactivity against VEGF, as depicted in Fig. 3 in green, exhibited an intense and uniformly distributed stippling pattern throughout the cytoplasm of motor neurons, excluding the cell nucleus. In Fig. 3, pictures of the immunohistochemical VEGF signal in the oculomotor, facial and hypoglossal nuclei are illustrated at 8, 12, and 16 weeks of age in both WT and SOD mice. VEGF immunolabelling in the abducens and trochlear nuclei is presented in Fig. S4. It is notable that the VEGF signal appeared more pronounced in WT animals for all analyzed nuclei, particularly within extraocular motor neurons, in comparison to the facial and hypoglossal counterparts.

In the WT, expression of VEGF in the oculomotor nuclei was more intense in the 8-week-old, followed by a non-significant decrease in the expression of the trophic factor at 12 and 16 weeks of age (Table 2). In contrast, the facial and hypoglossal nuclei showed *per se* a low expression of VEGF at all stages, compared to the three ocular nuclei. On the other hand, in SOD animals, VEGF expression was always lower than in WT animals in facial and hypoglossal nuclei. A striking observation was that in all the analyzed nuclei of SOD mice, the level of VEGF increased at the stage of 12 weeks with respect to the level observed at the onset stage of 8 weeks (†, $p < 0.001$; $F_{(2,60)}$: 8.61; Two-way–ANOVA test; factors: nuclei

and genotype; 8 *vs* 12 weeks), decreasing again at the final stage (16 weeks) (Fig. 4).

The statistical analysis of the VEGF intensity revealed that the level of VEGF was lower in all the brainstem nuclei of 8 weeks-old SOD mice compared to their respective WT control groups (*, $p < 0.05$; $F_{(1,40)}$: 80.12; Two-way-ANOVA test, factors: nuclei and genotype). In extraocular nuclei, at 12 and 16 weeks of survival, the VEGF level quantified in WT and SOD animals was similar. However, in the facial and hypoglossal nuclei, VEGF level remained always lower in the transgenic mice compared to their WT age-matched littermates (*, $p < 0.05$; 12 weeks: $F_{(1,40)}$: 32.82; 16 weeks: $F_{(1,40)}$: 21.52; Two-way-ANOVA test, factors: nuclei and genotype) (Table 2 and Fig. 4).

The bar diagram presented in Fig. 4 consistently illustrates that the three oculomotor nuclei always exhibited higher VEGF expression levels when compared to their respective values obtained in the facial and hypoglossal nuclei. Statistical analysis of the differential VEGF expression across all nuclei revealed that the VEGF levels were similar among the extraocular motor nuclei and significantly higher than those observed in the facial and hypoglossal nuclei at all stages of survival studied (#, $p < 0.001$; WT: $F_{(4,60)}$: 29.54; SOD: $F_{(4,60)}$: 22.97; Two-way–ANOVA test; factors: nuclei and time).

In summary, our findings indicated that the baseline VEGF levels were lower in brainstem motor neurons of SOD mice compared to their WT littermates in the initial stage. However, while these differences diminished to similar levels in the oculomotor nuclei during the progression of the disease, they persisted in the facial and hypoglossal nuclei. Furthermore, VEGF consistently displayed higher levels in extraocular motor neurons than in facial or hypoglossal motor neurons. Consequently, these differences in VEGF presence may contribute to the different survival rates between ocular and non-ocular motor neurons as the disease progresses.
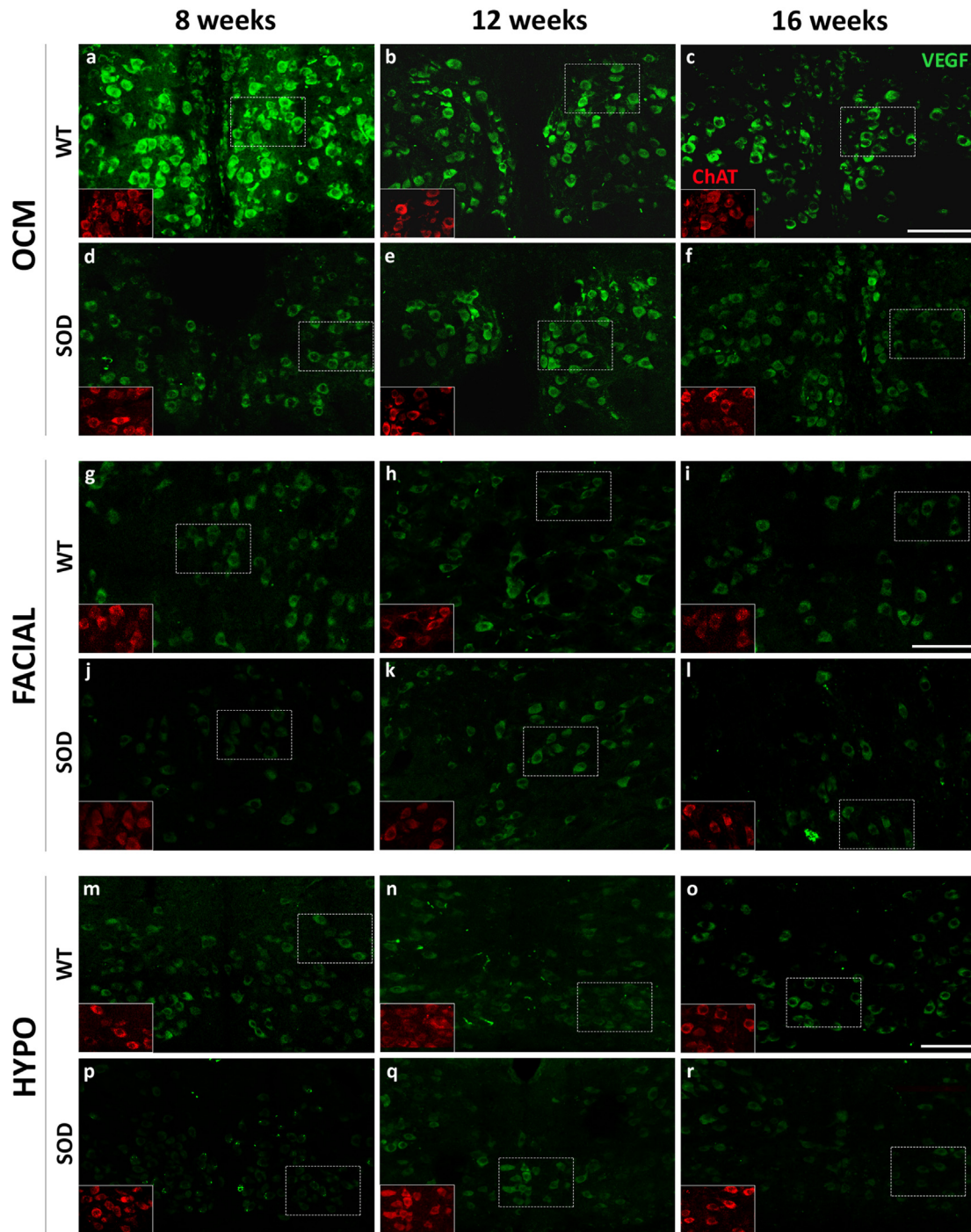
Fig. 3. Expression of VEGF in brainstem motor neurons. Confocal microscopy images showing the expression of VEGF (green) in the soma of the oculomotor (OCM), facial and hypoglossal (HYPO) motor neurons of WT (a-c, g-i and m-o) and SOD (d-f, j-l and p-r) mice at different survival times (8 weeks [a, d, g, j, m, p], 12 weeks [b, e, h, k, n, q] and 16 weeks [c, f, i, l, o, r]). ChAT signal (red in the inserts) was used to identify motor neurons. ChAT-positive red motor neurons showed in the inserts correspond to VEGF-labelled green motor neurons boxed with dashed lines. Ocular motor neurons (a–f) showed an intense expression of VEGF in their somata at 8, 12 and 16 weeks in the WT (a, b and c) and SOD mice (d, e and f). Note the high VEGF expression observed at 12 weeks in the oculomotor nuclei of SOD mice (e). The facial (g–l) and hypoglossal (m–r) nuclei always showed lower labelling for VEGF than the oculomotor nucleus, particularly in the SOD mice (j-l; p-r). Calibration bars: 100 μm.

Localization of TDP-43 in brainstem motor neurons

As stated above, while normal TDP-43 is typically located within cellular nuclei, pathological inclusions tend to appear translocated to the cytoplasm in conditions such as ALS. Hence, our study aimed to investigate whether that mislocalization of the TDP-43 protein was present in the brainstem motor neurons included in this work.

Immunohistochemistry was performed to locate the protein TDP-43 within the motor neurons of the brainstem motor nuclei in both WT and SOD mice at the final stage of survival (16 weeks).

The monoclonal antibody (DB9) employed in this study was raised against human TDP-43. In order to validate its applicability in mouse tissue, first, the epitope detected by DB9 in human TDP-43 was mapped, by immunoblot analysis of recombinant proteins, to amino acid residues

Table 2
VEGF optical density in cell somata.

Nucleus	8 weeks		12 weeks		16 weeks	
	WT	SOD	WT	SOD	WT	SOD
ABD	32.85 ± 4.26	23.44 ± 0.93	22.25 ± 3.36	11.22 ± 1.60	17.53 ± 2.89	15.18 ± 2.43
TROC	32.83 ± 2.83	23.71 ± 1.29	24.77 ± 2.67	12.46 ± 3.20	16.86 ± 3.14	15.93 ± 2.43
OCM	27.17 ± 3.31	22.87 ± 1.55	21.54 ± 3.17	13.10 ± 1.86	18.63 ± 1.57	14.15 ± 0.84
FACIAL	13.41 ± 3.50	14.20 ± 0.80	10.04 ± 0.58	3.30 ± 0.16	7.72 ± 0.68	5.65 ± 0.78
HYPO	12.15 ± 1.82	14.08 ± 0.55	8.40 ± 0.41	3.88 ± 0.37	7.53 ± 0.66	5.83 ± 0.65

Optical density of VEGF immunohistochemistry in brainstem nuclei of WT and SOD mice at the different stages of survival. Data are expressed as mean ± standard error of the mean.

314–322 of the human TDP-43 protein. The epitope detected (GAFSIN-PAM) is conserved between the mouse and human TDP-43 proteins (Fig. S2). The DB9 antibody detects a single band of 43 kDa in cell extracts prepared from two human cell lines (Fig. S2–c) and a predominant band of 43 kDa corresponding to TDP-43 in mouse brain tissue, thereby confirming the specificity of the antibody (Fig. S2–d).

Double fluorescent immunohistochemistry was performed on brainstem tissue collected from 16-weeks-old mice of both genotypes, targeting TDP-43 and ChAT, to investigate the subcellular localization of the TDP-43 protein. Our confocal analysis yielded no evidence of TDP-43 protein translocation from the cell nucleus to the cytoplasm within motor neurons of the brainstem nuclei at 16 weeks of age, irrespective of whether the mice were of the WT or SOD genotype. Representative confocal images in Fig. 5 depict the oculomotor, facial, and hypoglossal nuclei of both genotypes, where the TDP-43 signal (red) consistently remains confined to the cellular nuclei. Notably, no colocalization was observed between the TDP-43 and ChAT (green) signals, with the latter localized in the cytoplasm, a pattern consistent in both WT and SOD mice. Therefore, no quantitative analysis could be conducted due to the absence of any sign of TDP-43 translocation to the cytoplasm. Subsequently, we quantified the optical density of the TDP-43 labelling

localized in the nuclei of motor neurons, and no significant differences were found between resistant and vulnerable motor neurons at 16 weeks in SOD mice ($p > 0.05$; $F_{(4,10)}$: 0.93; One-way-ANOVA test, factor: nuclei).

Consequently, these findings suggest the absence of cytoplasmic translocation of TDP-43 within the brainstem motor neurons of this SOD model, even in the vulnerable pools at an advanced stage of the disease.

Discussion

The principal aim of this study was to investigate the survival dynamics of motor neurons in different brainstem motor nuclei throughout the course of disease progression in both WT and SOD mice, a well-established murine model of ALS, and to determine whether the expression of VEGF was associated with an enhanced resistance of specific motor neuron populations against neurodegeneration. Our results have, for the first time, revealed a positive correlation between VEGF levels within brainstem motor neurons and their resistance to degeneration in ALS. These findings suggest that the resilience of brainstem motor neurons in ALS disease may depend on the availability of VEGF.
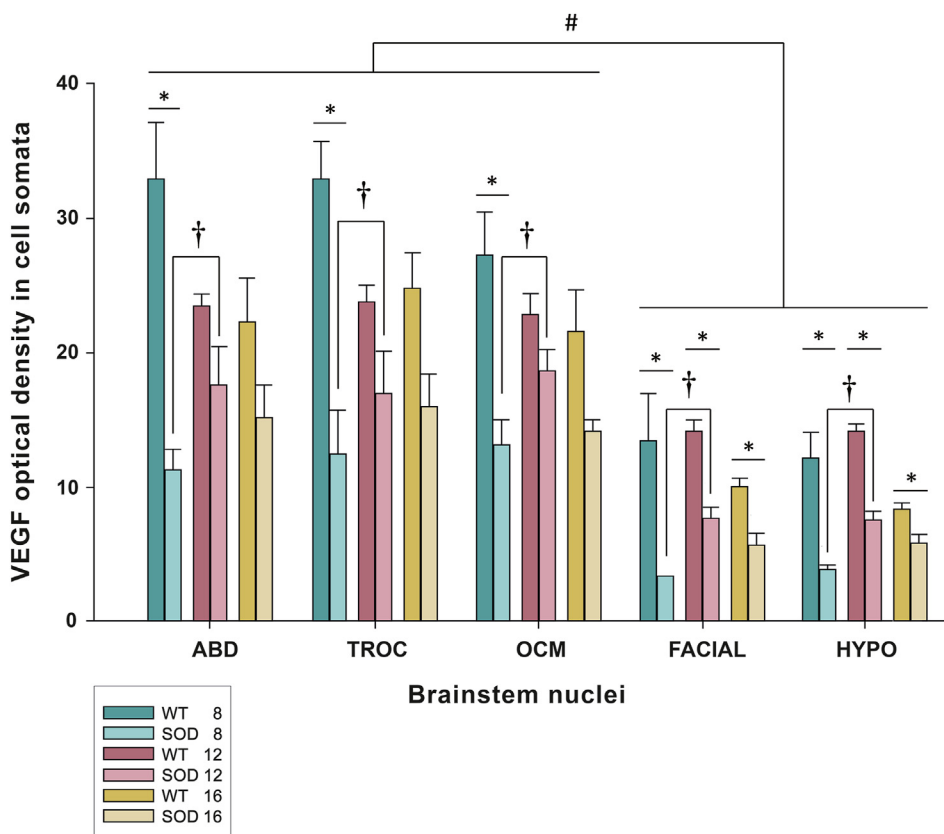

Fig. 4. Quantification of VEGF expression in the motor neurons of the brainstem motor nuclei of the WT and SOD mice at different stages of survival. The bar diagram illustrates the optical density of VEGF in the three ocular motor nuclei (ABD: abducens; TROC: trochlear; OCM: oculomotor) and in facial and hypoglossal (HYPO) nuclei at 8, 12 and 16 weeks in both genotypes (WT and SOD). Data represent mean ± SEM. Asterisks (*) represent significant differences between the WT and SOD strains of the five motor nuclei (One-way-ANOVA test; *, $p < 0.05$). Note that the facial and hypoglossal nuclei always presented a lower expression of VEGF in the SOD strain concerning the values quantified in their WT littermates. Daggers (†) indicate significant differences in VEGF expression between 8- and 12-weeks old on SOD mice (Two-way ANOVA test, Holm-Sidak method for multiple *post hoc* comparisons; †, $p < 0.001$). Hash marks (#) represent significant differences in the expression of VEGF between extraocular and non-extraocular (facial and hypoglossal) motor neurons (Two-way ANOVA test, Holm-Sidak method for multiple *post hoc* comparisons; #, $p < 0.001$). Note the higher expression of VEGF in the three oculomotor nuclei in the WT and SOD strains at any time with respect to the facial or hypoglossal nuclei.
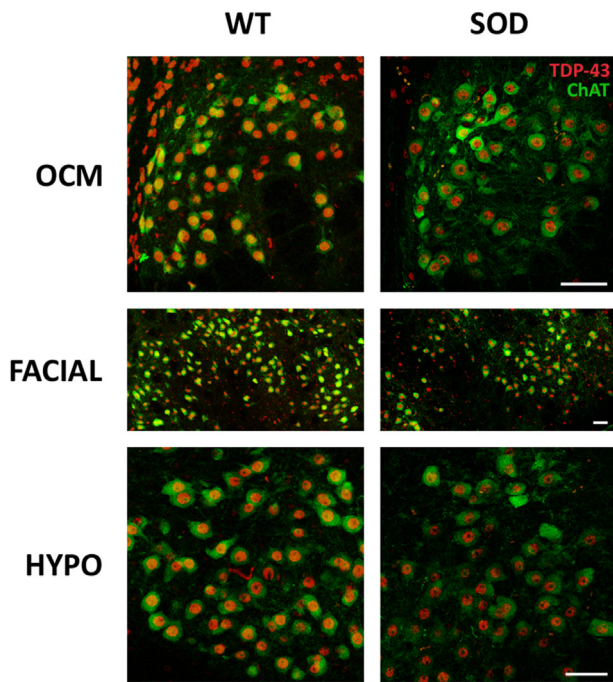
Fig. 5. Localization of TDP-43 in brainstem motor neurons. Confocal microscopy images showing the localization of the TDP-43 protein (in red) in the nucleus of the oculomotor (OCM), facial and hypoglossal (HYPO) motor neurons of 16-weeks-old SOD mice. The ChAT immunohistochemistry was used to label the cytoplasm of motor neurons (in green). Note that the TDP-43 signal was always located in the nucleus, showing the absence of any cytoplasmic translocation in brainstem motor neurons of SOD mice. Calibration bars: 50 μm.

Different survival rates of brainstem motor neurons in ALS model

One of the primary objectives of this project was to determine the number of motor neurons within the different brainstem motor nuclei at three selected survival stages (pre-symptomatic, onset, and end-stage) using the ALS murine model, to investigate potential variations in the survival rates among different motor neuron pools. Notably, a statistically significant decline in motor neuron numbers was observed solely in the facial and hypoglossal nuclei at both progression and end-stage (12 and 16 weeks of age). These findings agree with previous reports in the literature [6,9,10,12].

It is widely acknowledged that susceptibility to the disease varies among motor neurons, with those of the ocular motor system exhibiting notable resistance. This heightened resilience has been observed in humans, where ocular movements are preserved until the advanced stages of ALS [10], although some impairment may occur [53]. Moreover, this resistance has been found to be contingent on the specific mouse model of the disease. Notably, while the *pmn* mouse model displays oculomotor degeneration, this phenomenon is absent in *wobbler* and SODG93A mice, with the latter closely mirroring the symptomatic presentation of human ALS [6].

Consistently, our investigation revealed no significant loss of motor neurons within any of the three oculomotor nuclei in the SOD mice. Previous studies employed a similar methodology to quantify the survival of ocular motor neurons [6,12], although they focused solely on the oculomotor and trochlear nuclei, both oculomotor nuclei collectively referred to as the "oculomotor complex", not including the abducens nucleus. In these previous studies, the quantified neuronal loss within the oculomotor complex was found to be nonsignificant, accounting for less than 10%, a result consistent with our own findings. However, they reported a substantial loss ranging from 22% to 46% within the facial nucleus of SOD mice at the end-stage. This decline aligns closely with our study, where we observed an approximately 26% reduction in neuronal

count in 16-week-old SOD mice. Regarding the hypoglossal nucleus, our results demonstrated a higher percentage of neuronal loss, nearly 40%, which contrasts with earlier investigations reporting a maximum motoneuronal loss of 28% by the end-stage of the disease in the same mouse model to ours [6]. By the end-stage, surviving facial and hypoglossal motor neurons displayed signs of atrophy and vacuolar degeneration, except within the oculomotor nuclei. It is also important to acknowledge that different mouse models of ALS may exhibit slight variations in their motoneuronal survival rates [6,12].

The underlying reasons for this varying vulnerability remain elusive to date. Nonetheless, there exist several hypotheses and factors that may, at least partially, account for the observed differences in motor neuron survival among the populations under investigation.

VEGF expression in brainstem nuclei and its relationship with ALS

The different vulnerability of motoneuronal pools in ALS has been associated with several factors (as reviewed in Ref. [33]). Resistant ocular motor neurons exhibit a distinct protein signature, characterized by a higher presence of calcium-binding proteins like parvalbumin, GABA receptor Gabra1, neuropeptide PACAP, and IGF-2, coupled with lower levels of dynein or peripherin [9,14,54–59]. Furthermore, notable disparities exist in the muscles and neuromuscular junction (revised in Ref. [33]) between the extraocular and other motor systems [10,60–64].

In extraocular muscles, preservation of neurotrophic factors during the neurodegenerative progression associated with ALS has been suggested to be relevant for their resistance [61]. Numerous trophic factors have been associated with survival, including the neurotrophin family, GDNF, or CNTF [65–70] However, several clinical trials in patients with this pathology who have been provided with trophic factors subcutaneously have not produced the desired effects to date [71,72]. Notably, it has been the neurotrophic factor VEGF that has raised more expectations in the last two decades in the context of ALS-related neurodegeneration [18,19,73].

The role of VEGF as a neuroprotective factor for motor neurons has been extensively explored, particularly following the publication of the study by Oosthuyse et al., since it was the first to establish a direct connection between low levels of VEGF and motor neuron degeneration [18]. This statement is supported by other studies where VEGF in ALS mouse models demonstrated a delay in the disease course [23,70,74,75]. In additional studies, SOD mice crossbred with mice overexpressing VEGF (VEGF$^{+/+}$) resulted in increased motor neuron survival [76,77]. More recently, higher levels of VEGF expression have been described in rat oculomotor nuclei in a control situation, compared to other non-oculomotor nuclei in the brainstem [34].

However, VEGF expression in motor neurons located in the brainstem of the SOD^{G93A} has remained unexplored until now. Our study marks the first scientific endeavor addressing this matter, potentially shedding light on the selective resistance displayed by distinct motor neuron populations against the degenerative processes triggered during ALS.

Interestingly, the most significant finding of this study is that VEGF levels consistently remained higher in motor neurons of the ocular motor system than in those innervating the tongue and facial muscles. Reduced VEGF level has also been detected in the central nervous system and CSF of ALS patients [20,21,78]. Our results also indicated a baseline level of VEGF at 8 weeks of survival in all analyzed nuclei compared to their WT littermates. However, as the disease progressed, these differences disappeared in extraocular motor neurons, showing similar levels to those of control animals. The transient increase of VEGF during the initial stages of the degenerative process (12 weeks) may contribute to their enhanced survival (Fig. 6). In line with this, previous studies have reported the therapeutic potential of VEGF in delaying the progression of motor neuron loss occurring before the onset of motor symptoms [79]. Accordingly, transient hyperexcitability has been detected in hypoglossal motor neurons of mice in the initial symptomatic stage, but not in the end-stage [80], associating this phenomenon with the remodelling of
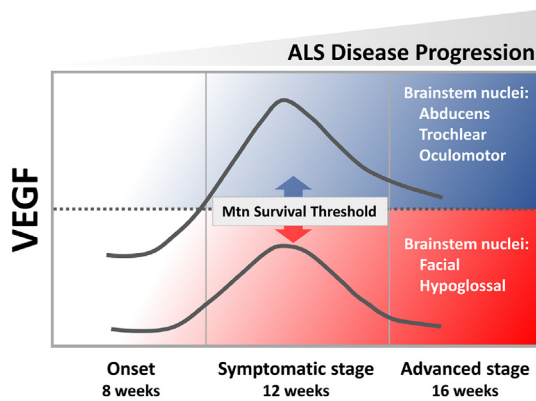
Fig. 6. Scheme summarizing the VEGF level observed in the different pools of brainstem motor neurons and its relationship with motoneuronal survival along the disease progression. Note that VEGF was consistently higher in motor neurons of the oculomotor system (resistant) regarding the level observed in motor neurons of the facial and the hypoglossal motor systems (vulnerable in ALS disease).

Ca^{2+} handling, being that time frame when the motor neurons are more vulnerable. Likewise, the fact that VEGF levels always remained lower in the non-oculomotor neurons of the SOD mice compared to WT levels could explain why these motoneuronal pools are more susceptible and why the degenerative process begins earlier.

In light of our findings, it can be postulated that the heightened resilience exhibited by ocular motor neurons may, in part, be attributable to the neuroprotective role played by VEGF thanks to its ability to mitigate excitotoxic processes by modulating the transcription of the GluA2 subunit within AMPA receptors [81]. That influence reduces Ca^{2+} permeability, which is significant given the pronounced susceptibility of motor neurons to excitotoxic stress [82] and their deficient expression of the GluA2 subunit [83–86]. Moreover, it is established that the neuroprotective effect of VEGF is mediated by VEGFR-2, activating the PI3K/Akt signaling pathway [87], inhibiting pro-apoptotic proteins, and inducing anti-apoptotic molecules [19,70,88–91]. Hence, the elevated VEGF expression in oculomotor neurons observed in our study may prompt an upregulation of anti-apoptotic proteins, potentially explaining their greater resistance to neurodegeneration. The promising role of VEGF in the treatment of ALS is such that clinical trials have already begun to assess its safety and bioavailability in the central nervous system of humans [92].

Therefore, our data support the notion that the elevated levels of VEGF observed in extraocular motor neurons may play a pivotal role in explaining their prolonged survival during the degenerative process associated with ALS.

Absence of TDP-43 cytoplasmic translocation in brainstem motor neurons of SOD1^{G93A} mice

Another objective of our work was to study the subcellular localization of TDP-43 in the motor neurons of the oculomotor and non-oculomotor nuclei of the brainstem of WT and SOD mice.

Redistribution of the nuclear protein TDP-43 to the cytoplasm in spinal motor neurons is a characteristic of human ALS pathology [39, 93–95] and may be associated with ubiquitinated or phosphorylated inclusions. Several lines of research have recently focused on the study of the abnormal distribution, and its effects, of TDP-43 as a part of the disease process of ALS [37,48] and other neurodegenerative diseases, such as FTLD and Alzheimer's disease [37,96,97]. An increased level of TDP-43 protein has also been observed in CSF of ALS patients [98,99], which makes it a promising biomarker for an early stage of the human disease. However, motor neurons of the oculomotor system, which are spared from degeneration, differ from vulnerable neurons because they

do not contain TDP-43 cytoplasmic aggregates, in contrast to other brainstem nuclei, including the facial and the hypoglossal nuclei [100]. Only in scarce advanced cases of the disease, the TDP-43 aggregates have been observed in the oculomotor nucleus [94]. In striking contrast, several studies performed in tissue from SOD1-related familial ALS patients found no cytoplasmic TDP-43 immunoreactivity [101], implicating different molecular mechanisms in sporadic and SOD1-related familial pathology in humans [39].

In agreement with those previously mentioned studies, TDP-43 redistribution was not observed in the spinal cord motor neurons of the SOD^{G93A} mice [43,44,70], suggesting that not all the biochemical alterations observed in humans could be presented in this transgenic mouse model of ALS [44]. However, other authors did find redistribution of TDP-43 to the cytoplasm of motor neurons in mutant SOD transgenic mice, but only those at an advanced disease [45,47,102,103].

Based on those antecedents, we aimed to know if TDP-43 mislocalization exhibited differential occurrence in brainstem motor neurons of the SOD mouse model, an area that had not been previously explored. Our study revealed no mislocalization of the TDP-43 protein from the cell nucleus to the cytoplasm in any of the motor neurons of the brainstem nuclei, neither in resistant nor in vulnerable with 16 weeks of age. Taking all these data together, it could be suggested that the translocation of TDP-43 to the cytoplasm is not a common event in all ALS models. Taking all these data together, it could be suggested that the translocation of TDP-43 to the cytoplasm is not a common event in all ALS models. Our findings, which reveal an absence of correlation between TDP-43 translocation and VEGF expression in motor neurons exhibiting varying susceptibility to degeneration in SOD mice, lead us to postulate that VEGF may indeed function as a reliable marker for the disease.

In conclusion, the most noteworthy discovery arising from this work is that resistant extraocular motor neurons exhibit a heightened expression of the neuroprotective factor VEGF when compared to the susceptible facial and hypoglossal motor neurons within the SOD^{G93A} mouse model of ALS. Consequently, the obtained data provides substantial support to the hypothesis positing that the presence of VEGF may be of critical importance in preserving motor neurons in the context of this disease. Therefore, we propose a direct positive correlation between the level of VEGF within brainstem motor neurons and their resistance to degeneration in ALS.

Author Contributions

Conceptualisation, S.M. and A.M.P.; methodology, S.S.H., M.E.F.d.S. and S.M.; data analysis, S.S.H., M.E.F.d.S. and S.M.; writing—original draft preparation, SM; writing—review and editing, S.S.H., M.E.F.d.S., A.M.P., F.E.B. and D.P.; project administration, A.M.P. and D.P.; generation and characterization of TDP-43 antibody, K.M.H. and F.E.B; maintenance of animals, J.M.F. and D.P.; All authors have read and agreed to the published version of the manuscript.

Data availability statement

Datasets can be provided by the corresponding authors upon a reasonable request.

Declaration of competing interest

The authors declare the following financial interests/personal relationships which may be considered as potential competing interests: Angel M Pastor reports financial support was provided by Government of Andalusia. Angel M Pastor reports financial support was provided by Ministry of Science Technology and Innovations. David Pozo reports financial support was provided by Ministry of Science Technology and Innovations. David Pozo reports financial support from the following foundations: CONTRA LA ELA (Reto Todos Unidos), Fundació Catalana d'ELA Miquel Valls, and Juntos Contra la ELA. If there are other authors,

they declare that they have no known competing financial interests or personal relationships that could have appeared to influence the work reported in this paper.

Appendix A. Supplementary data

Supplementary data to this article can be found online at https://doi.org/10.1016/j.neurot.2024.e00340.

References

[1] Norris SP, Likanje M-FN, Andrews JA. Amyotrophic lateral sclerosis: update on clinical management. Curr Opin Neurol 2020;33:641–8. https://doi.org/10.1097/WCO.0000000000000864.

[2] van Es MA, Hardiman O, Chio A, Al-Chalabi A, Pasterkamp RJ, Veldink JH, et al. Amyotrophic lateral sclerosis. Lancet 2017;390:2084–98. https://doi.org/10.1016/S0140-6736(17)31287-4.

[3] Caballero-Hernandez D, Toscano MG, Cejudo-Guillen M, Garcia-Martin ML, Lopez S, Franco JM, et al. The "omics" of amyotrophic lateral sclerosis. Trends Mol Med 2016;22:53–67. https://doi.org/10.1016/j.molmed.2015.11.001.

[4] Fisher EMC, Greensmith L, Malaspina A, Fratta P, Hanna MG, Schiavo G, et al. Opinion: more mouse models and more translation needed for ALS. Mol Neurodegener 2023;18(1):30. https://doi.org/10.1186/s13024-023-00619-2.

[5] Cirulli ET, Lasseigne BN, Petrovski S, Sapp PC, Dion PA, Leblond CS, et al. Exome sequencing in amyotrophic lateral sclerosis identifies risk genes and pathways. Science 2015;347:1436–41. https://doi.org/10.1126/science.aaa3650.

[6] Haenggeli C, Kato AC. Differential vulnerability of cranial motoneurons in mouse models with motor neuron degeneration. Neurosci Lett 2002;335:39–43. https://doi.org/10.1016/s0304-3940(02)01140-0.

[7] Gurney ME, Pu H, Chiu AY, Dal Canto MC, Polchow CY, Alexander DD, et al. Motor neuron degeneration in mice that express a human Cu,Zn superoxide dismutase mutation. Science 1994;264:1772–5. https://doi.org/10.1126/science.8209258.

[8] Bennett EJ, Mead RJ, Azzouz M, Shaw PJ, Grierson AJ. Early detection of motor dysfunction in the SOD1G93A mouse model of amyotrophic lateral sclerosis (ALS) using home cage running wheels. PLoS One 2014;9. https://doi.org/10.1371/journal.pone.0107918.

[9] Comley L, Allodi I, Nichterwitz S, Nizzardo M, Simone C, Corti S, et al. Motor neurons with differential vulnerability to degeneration show distinct protein signatures in health and ALS. Neuroscience 2015;291:216–29. https://doi.org/10.1016/j.neuroscience.2015.02.013.

[10] Nijssen J, Comley LH, Hedlund E. Motor neuron vulnerability and resistance in amyotrophic lateral sclerosis. Acta Neuropathol 2017;133:863–85. https://doi.org/10.1007/s00401-017-1708-8.

[11] Allodi I, Nijssen J, Benitez JA, Schweingruber C, Fuchs A, Bonvicini G, et al. Modeling motor neuron resilience in ALS using stem cells. Stem Cell Rep 2019;12:1329–41. https://doi.org/10.1016/j.stemcr.2019.04.009.

[12] Nimchinsky EA, Young WG, Yeung G, Shah RA, Gordon JW, Bloom FE, et al. Differential vulnerability of oculomotor, facial, and hypoglossal nuclei in G86R superoxide dismutase transgenic mice. J Comp Neurol 2000;416:112–25. https://doi.org/10.1002/(SICI)1096-9861(20000103)416:1<112::AID-CNE9>3.0.CO;2-K.

[13] DePaul R, Abbs JH, Caligiuri M, Gracco VL, Brooks BR. Hypoglossal, trigeminal, and facial motoneuron involvement in amyotrophic lateral sclerosis. Neurology 1988;38:281–3. https://doi.org/10.1212/wnl.38.2.281.

[14] Reiner A, Medina L, Figueredo-Cardenas G, Anfinson S. Brainstem motoneuron pools that are selectively resistant in amyotrophic lateral sclerosis are preferentially enriched in parvalbumin: evidence from monkey brainstem for a calcium-mediated mechanism in sporadic ALS. Exp Neurol 1995;131:239–50. https://doi.org/10.1016/0014-4886(95)90046-2.

[15] Sathasivam S. VEGF and ALS. Neurosci Res 2008;62:71–7. https://doi.org/10.1016/j.neures.2008.06.008.

[16] Lu L, Zheng L, Viera L, Suswam E, Li Y, Li X, et al. Mutant Cu/Zn-superoxide dismutase associated with amyotrophic lateral sclerosis destabilizes vascular endothelial growth factor mRNA and downregulates its expression. J Neurosci 2007;27:7929–38. https://doi.org/10.1523/JNEUROSCI.1877-07.2007.

[17] Storkebaum E, Carmeliet P. VEGF: a critical player in neurodegeneration. J Clin Invest 2004;113:14–8. https://doi.org/10.1172/JCI200420682.

[18] Oosthuyse B, Moons L, Storkebaum E, Beck H, Nuyens D, Brusselmans K, et al. Deletion of the hypoxia-response element in the vascular endothelial growth factor promoter causes motor neuron degeneration. Nat Genet 2001;28:131–8. https://doi.org/10.1038/88842.

[19] Lunn JS, Sakowski SA, Kim B, Rosenberg AA, Feldman EL. Vascular endothelial growth factor prevents G93A-SOD1-induced motor neuron degeneration. Dev Neurobiol 2009;69:871–84. https://doi.org/10.1002/dneu.20747.

[20] Brockington A, Wharton SB, Fernando M, Gelsthorpe CH, Baxter L, Ince PG, et al. Expression of vascular endothelial growth factor and its receptors in the central nervous system in amyotrophic lateral sclerosis. J Neuropathol Exp Neurol 2006;65:26–36. https://doi.org/10.1097/01.jnen.0000196134.51217.74.

[21] Devos D, Moreau C, Lassalle P, Perez T, De Seze J, Brunaud-Danel V, et al. Low levels of the vascular endothelial growth factor in CSF from early ALS patients. Neurology 2004;62:2127–9. https://doi.org/10.1212/01.wnl.0000129913.44351.a3.

[22] Khosla R, Rain M, Chawathey S, Modgil S, Tyagi R, Thakur K, et al. Identifying putative cerebrospinal fluid biomarkers of amyotrophic lateral sclerosis in a north Indian population. Muscle Nerve 2020;62:528–33. https://doi.org/10.1002/mus.27026.

[23] Azzouz M, Ralph GS, Storkebaum E, Walmsley LE, Mitrophanous KA, Kingsman SM, et al. VEGF delivery with retrogradely transported lentivector prolongs survival in a mouse ALS model. Nature 2004;429:413–7. https://doi.org/10.1038/nature02544.

[24] Dukkipati SS, Garrett TL, Elbasiouny SM. The vulnerability of spinal motoneurons and soma size plasticity in a mouse model of amyotrophic lateral sclerosis. J Physiol 2018;596:1723–45. https://doi.org/10.1113/JP275498.

[25] Watabe K, Ohashi T, Sakamoto T, Kawazoe Y, Takeshima T, Oyanagi K, et al. Rescue of lesioned adult rat spinal motoneurons by adenoviral gene transfer of glial cell line-derived neurotrophic factor. J Neurosci Res 2000;60:511–9. https://doi.org/10.1002/(SICI)1097-4547(20000515)60:4<511::AID-JNR10>3.0.CO;2-I.

[26] Bravo-Hernandez M, Tadokoro T, Navarro MR, Platoshyn O, Kobayashi Y, Marsala S, et al. Spinal subpial delivery of AAV9 enables widespread gene silencing and blocks motoneuron degeneration in ALS. Nat Med 2020;26:118–30. https://doi.org/10.1038/s41591-019-0674-1.

[27] Ohgomori T, Yamasaki R, Takeuchi H, Kadomatsu K, Kira JI, Jinno S. Differential activation of neuronal and glial STAT3 in the spinal cord of the SOD1G93A mouse model of amyotrophic lateral sclerosis. Eur J Neurosci 2017;46:2001–14. https://doi.org/10.1111/ejn.13650.

[28] Kang BH, Kim J Il, Lim YM, Kim KK. Abnormal oculomotor functions in amyotrophic lateral sclerosis. J Clin Neurol 2018;14:464–71. https://doi.org/10.3988/jcn.2018.14.4.464.

[29] Chang Q, Martin LJ. Voltage-gated calcium channels are abnormal in cultured spinal motoneurons in the G93A-SOD1 transgenic mouse model of ALS. Neurobiol Dis 2016;93:78–95. https://doi.org/10.1016/j.nbd.2016.04.009.

[30] Bede P, Chipika RH, Finegan E, Li Hi Shing S, Doherty MA, Hengeveld JC, et al. Brainstem pathology in amyotrophic lateral sclerosis and primary lateral sclerosis: a longitudinal neuroimaging study. NeuroImage Clin 2019;24:102054. https://doi.org/10.1016/j.nicl.2019.102054.

[31] Ferrucci M, Spalloni A, Bartalucci A, Cantafora E, Fulceri F, Nutini M, et al. A systematic study of brainstem motor nuclei in a mouse model of ALS, the effects of lithium. Neurobiol Dis 2010;37:370–83. https://doi.org/10.1016/j.nbd.2009.10.017.

[32] Benítez-Temiño B, Davis-López de Carrizosa MA, Morcuende S, Matarredona ER, de la Cruz RR, Pastor AM. Functional diversity of neurotrophin actions on the oculomotor system. Int J Mol Sci 2016;17:2016. https://doi.org/10.3390/ijms17122016.

[33] Silva-Hucha S, Pastor AM, Morcuende S. Neuroprotective effect of vascular endothelial growth factor on motoneurons of the oculomotor system. Int J Mol Sci 2021;22:814. https://doi.org/10.3390/ijms22020814.

[34] Silva-Hucha S, Hernández RG, Benítez-Temiño B, Pastor AM, de la Cruz RR, Morcuende S. Extraocular motoneurons of the adult rat show higher levels of vascular endothelial growth factor and its receptor Flk-1 than other cranial motoneurons. PLoS One 2017;12:e0178616. https://doi.org/10.1371/journal.pone.0178616.

[35] Silva-Hucha S, Carrero-Rojas G, Fernández de Sevilla ME, Benítez-Temiño B, Davis-López de Carrizosa MA, Pastor AM, et al. Sources and lesion-induced changes of VEGF expression in brainstem motoneurons. Brain Struct Funct 2020. https://doi.org/10.1007/s00429-020-02057-y.

[36] Neumann M, Sampathu DM, Kwong LK, Truax AC, Micsenyi MC, Chou TT, et al. Ubiquitinated TDP-43 in frontotemporal lobar degeneration and amyotrophic

lateral sclerosis. Science 2006;314:130–3. https://doi.org/10.1126/science.1134108.

[37] Arai T, Hasegawa M, Akiyama H, Ikeda K, Nonaka T, Mori H, et al. TDP-43 is a component of ubiquitin-positive tau-negative inclusions in frontotemporal lobar degeneration and amyotrophic lateral sclerosis. Biochem Biophys Res Commun 2006;351:602–11. https://doi.org/10.1016/j.bbrc.2006.10.093.

[38] Eisen A. The dying forward hypothesis of ALS: tracing its history. Brain Sci 2021; 11:300. https://doi.org/10.3390/brainsci11030300.

[39] Mackenzie IRA, Bigio EH, Ince PG, Geser F, Neumann M, Cairns NJ, et al. Pathological TDP-43 distinguishes sporadic amyotrophic lateral sclerosis from amyotrophic lateral sclerosis with SOD1 mutations. Ann Neurol 2007;61:427–34. https://doi.org/10.1002/ana.21147.

[40] Asakawa K, Handa H, Kawakami K. Multi-phaseted problems of TDP-43 in selective neuronal vulnerability in ALS. Cell Mol Life Sci 2021;78:4453–65. https://doi.org/10.1007/s00018-021-03792-z.

[41] Highley JR, Kirby J, Jansweijer JA, Webb PS, Hewamadduma CA, Heath PR, et al. Loss of nuclear TDP-43 in amyotrophic lateral sclerosis (ALS) causes altered expression of splicing machinery and widespread dysregulation of RNA splicing in motor neurones. Neuropathol Appl Neurobiol 2014;40:670–85. https://doi.org/10.1111/nan.12148.

[42] Dickson DW, Josephs KA, Amador-Ortiz C. TDP-43 in differential diagnosis of motor neuron disorders. Acta Neuropathol 2007;114:71–9. https://doi.org/10.1007/s00401-007-0234-5.

[43] Robertson J, Sanelli T, Xiao S, Yang W, Horne P, Hammond R, et al. Lack of TDP-43 abnormalities in mutant SOD1 transgenic mice shows disparity with ALS. Neurosci Lett 2007;420:128–32. https://doi.org/10.1016/j.neulet.2007.03.066.

[44] Turner BJ, Baumer D, Parkinson NJ, Scaber J, Ansorge O, Talbot K, et al. TDP-43 expression in mouse models of amyotrophic lateral sclerosis and spinal muscular atrophy. BMC Neurosci 2008;9:104. https://doi.org/10.1186/1471-2202-9-104.

[45] Shan X, Vocadlo D, Krieger C. Mislocalization of TDP-43 in the G93A mutant SOD1 transgenic mouse model of ALS. Neurosci Lett 2009;458:70–4. https://doi.org/10.1016/j.neulet.2009.04.031.

[46] Cai M, Lee K-W, Choi S-M, Yang EJ. TDP-43 modification in the hSOD1G93A amyotrophic lateral sclerosis mouse model. 2014. https://doi.org/10.1179/17431 32814Y.0000000443.

[47] Lu Y, Tang C, Zhu L, Li J, Liang H, Zhang J, et al. The overexpression of TDP-43 protein in the neuron and oligodendrocyte cells causes the progressive motor neuron degeneration in the SOD1 G93A transgenic mouse model of amyotrophic lateral sclerosis. Int J Biol Sci 2016;12:1140–9. https://doi.org/10.7150/ijbs.15938.

[48] Leal-Lasarte MM, Franco JM, Labrador-Garrido A, Pozo D, Roodveldt C. Extracellular TDP-43 aggregates target MAPK/MAK/MRK overlapping kinase (MOK) and trigger caspase-3/IL-18 signaling in microglia. FASEB J 2017: fj.201601163R. https://doi.org/10.1096/fj.201601163R.

[49] Pérez-Cabello JA, Silvera-Carrasco L, Franco JM, Capilla-González V, Armaos A, Gómez-Lima M, et al. MAPK/MAK/MRK overlapping kinase (MOK) controls microglial inflammatory/type-I IFN responses via Brd4 and is involved in ALS. Proc Natl Acad Sci U S A 2023;120(28):e2302143120. https://doi.org/10.1073/pnas.2302143120.

[50] Shantanu S, Vijayalakshmi K, Shruthi S, Sagar BKC, Sathyaprabha TNN, Nalini A, et al. VEGF alleviates ALS-CSF induced cytoplasmic accumulations of TDP-43 and FUS/TLS in NSC-34 cells. J Chem Neuroanat 2017;81:48–52. https://doi.org/10.1016/j.jchemneu.2017.01.007.

[51] Schmitz C, Hof PR. Design-based stereology in neuroscience. Neuroscience 2005; 130:813–31. https://doi.org/10.1016/j.neuroscience.2004.08.050.

[52] Toft MH, Gredal O, Pakkenberg B. The size distribution of neurons in the motor cortex in amyotrophic lateral sclerosis. J Anat 2005;207:399–407. https://doi.org/10.1111/j.1469-7580.2005.00465.x.

[53] Sharma R, Hicks S, Berna CM, Kennard C, Talbot K, Turner MR. Oculomotor dysfunction in amyotrophic lateral sclerosis. Arch Neurol 2011;68:857–61. https://doi.org/10.1001/archneurol.2011.130.

[54] Allodi I, Comley L, Nichterwitz S, Nizzardo M, Simone C, Aguila Benitez J, et al. Differential neuronal vulnerability identifies IGF-2 as a protective factor in ALS and SMA. Nat Publ Gr 2016:1–39. https://doi.org/10.1038/srep25960.

[55] Maugeri G, D'Amico AG, Morello G, Reglodi D, Cavallaro S, D'Agata V. Differential vulnerability of oculomotor versus hypoglossal nucleus during ALS: involvement of PACAP. Front Neurosci 2020;14:1–10. https://doi.org/10.3389/fnins.2020.00805.

[56] Hedlund E, Karlsson M, Osborn T, Ludwig W, Isacson O. Global gene expression profiling of somatic motor neuron populations with different vulnerability identify molecules and pathways of degeneration and protection. Brain 2010;133: 2313–30. https://doi.org/10.1093/brain/awq167.

[57] Brockington A, Ning K, Heath PR, Wood E, Kirby J, Fusi N, et al. Unravelling the enigma of selective vulnerability in neurodegeneration: motor neurons resistant to degeneration in ALS show distinct gene expression characteristics and decreased susceptibility to excitotoxicity. Acta Neuropathol 2013;125:95–109. https://doi.org/10.1007/s00401-012-1058-5.

[58] Laslo P, Lipski J, Nicholson LF, Miles GB, Funk GD. Calcium binding proteins in motoneurons at low and high risk for degeneration in ALS. Neuroreport 2000;11: 3305–8. https://doi.org/10.1097/00001756-200010200-00009.

[59] Sasaki S, Warita H, Komori T, Murakami T, Abe K, Iwata M. Parvalbumin and calbindin D-28k immunoreactivity in transgenic mice with a G93A mutant SOD1 gene. Brain Res 2006;1083:196–203. https://doi.org/10.1016/j.brainres.2006.01.129.

[60] Harandi VM, Lindquist S, Kolan SS, Brännström T, Liu JX. Analysis of neurotrophic factors in limb and extraocular muscles of mouse model of amyotrophic lateral

sclerosis. PLoS One 2014;9:e109833. https://doi.org/10.1371/journal.pone.0109833.

[61] Harandi VM, Gaied ARN, Brännström T, Pedrosa Domellöf F, Liu J-X. Unchanged neurotrophic factors and their receptors correlate with sparing in extraocular muscles in amyotrophic lateral sclerosis. Invest Ophthalmol Vis Sci 2016;57: 6831–42. https://doi.org/10.1167/iovs.16-20074.

[62] Zimmermann L, Morado-Díaz CJ, Davis-López de Carrizosa MA, de la Cruz RR, May PJ, Streicher J, et al. Axons giving rise to the palisade endings of feline extraocular muscles display motor features. J Neurosci 2013;33:2784–93. https://doi.org/10.1523/JNEUROSCI.4116-12.2013.

[63] Büttner-Ennever JA, Horn AK, Scherberger H, D'Ascanio P. Motoneurons of twitch and nontwitch extraocular muscle fibers in the abducens, trochlear, and oculomotor nuclei of monkeys. J Comp Neurol 2001;438:318–35. https://doi.org/10.1002/cne.1318.

[64] Tjust AE, Brannstrom T, Pedrosa-Domellöf F, Pedrosa Domellof F. Unaffected motor endplate occupancy in eye muscles of ALS G93A mouse model. Front Biosci 2012:1547–55. https://doi.org/10.1109/epqu.2011.6128966.

[65] Oppenheim RW. Neurotrophic survival molecules for motoneurons: an embarrassment of riches. Neuron 1996;17:195–7. https://doi.org/10.1016/S0896-6273(00)80151-8.

[66] Henderson CE, Yamamoto Y, Livet J, Arce V, Garces A, DeLapeyrière O. Role of neurotrophic factors in motoneuronal development. J Physiol 1998;92:279–81. https://doi.org/10.1016/0168-9525(88)90137-0.

[67] Carmeliet P, Storkebaum E. Vascular and neuronal effects of VEGF in the nervous system: implications for neurological disorders. Semin Cell Dev Biol 2002;13: 39–53. https://doi.org/10.1006/scdb.2001.0290.

[68] Tolosa L, Mir M, Asensio VJ, Olmos G, Lladó J. Vascular endothelial growth factor protects spinal cord motoneurons against glutamate-induced excitotoxicity via phosphatidylinositol 3-kinase. J Neurochem 2008;105:1080–90. https://doi.org/10.1111/j.1471-4159.2007.05206.x.

[69] Gould TW, Oppenheim RW. Motor neuron trophic factors: therapeutic use in ALS? Brain Res Rev 2011;67:1–39. https://doi.org/10.1016/j.brainresrev.2010.10.003.

[70] Tovar-y-Romo LB, Ramírez-Jarquín UN, Lazo-Gómez R, Tapia R. Trophic factors as modulators of motor neuron physiology and survival: implications for ALS therapy. Front Cell Neurosci 2014;8:61. https://doi.org/10.3389/fncel.2014.00061.

[71] Henriques A, Pitzer C, Schneider A. Neurotrophic growth factors for the treatment of amyotrophic lateral sclerosis: where do we stand? Front Neurosci 2010;4:1–14. https://doi.org/10.3389/fnins.2010.00032.

[72] Keifer OP, O'Connor DM, Boulis NM. Gene and protein therapies utilizing VEGF for ALS. Pharmacol Ther 2014;141:261–71. https://doi.org/10.1016/j.pharmthera.2013.10.009.

[73] Tovar-y-Romo LB, Zepeda A, Tapia R. Vascular endothelial growth factor prevents paralysis and motoneuron death in a rat model of excitotoxic spinal cord neurodegeneration. J Neuropathol Exp Neurol 2007;66:913–22. https://doi.org/10.1097/nen.0b013e3181567c16.

[74] Storkebaum E, Lambrechts D, Dewerchin M, Moreno-Murciano MP, Appelmans S, Oh H, et al. Treatment of motoneuron degeneration by intracerebroventricular delivery of VEGF in a rat model of ALS. Nat Neurosci 2005;8:85–92. https://doi.org/10.1038/nn1360.

[75] Zheng C, Nennesmo I, Fadeel B, Henter JI. Vascular endothelial growth factor prolongs survival in a transgenic mouse model of ALS. Ann Neurol 2004;56: 564–7. https://doi.org/10.1002/ana.20223.

[76] Lambrechts D, Storkebaum E, Morimoto M, Del-Favero J, Desmet F, Marklund SL, et al. VEGF is a modifier of amyotrophic lateral sclerosis in mice and humans and protects motoneurons against ischemic death. Nat Genet 2003;34:383–94. https://doi.org/10.1038/ng1211.

[77] Wang Y, Mao XO, Xie L, Banwait S, Marti HH, Greenberg DA, et al. Vascular endothelial growth factor overexpression delays neurodegeneration and prolongs survival in amyotrophic lateral sclerosis mice. J Neurosci 2007;27:304–7. https://doi.org/10.1523/JNEUROSCI.4433-06.2007.

[78] Gao L, Zhou S, Cai H, Gong Z, Zang D. VEGF levels in CSF and serum in mild ALS patients. J Neurol Sci 2014;346:216–20. https://doi.org/10.1016/j.jns.2014.08.031.

[79] Tovar-y-Romo LB, Tapia R. Delayed administration of VEGF rescues spinal motor neurons from death with a short effective time frame in excitotoxic experimental models in vivo. ASN Neuro 2012;4:121–9. https://doi.org/10.1042/AN20110057.

[80] Fuchs A, Kutterer S, Mühling T, Duda J, Schütz B, Liss B, et al. Selective mitochondrial Ca2+ uptake deficit in disease endstage vulnerable motoneurons of the SOD1G93A mouse model of amyotrophic lateral sclerosis. J Physiol 2013;591: 2723–45. https://doi.org/10.1113/jphysiol.2012.247981.

[81] Bogaert E, Van Damme P, Poesen K, Dhondt J, Hersmus N, Kiraly D, et al. VEGF protects motor neurons against excitotoxicity by upregulation of GluR2. Neurobiol Aging 2010;31:2185–91. https://doi.org/10.1016/j.neurobiolaging.2008.12.007.

[82] Van Den Bosch L, Robberecht W. Different receptors mediate motor neuron death induced by short and long exposures to excitotoxicity. Brain Res Bull 2000;53: 383–8. https://doi.org/10.1016/S0361-9230(00)00371-3.

[83] Van Damme P, Van Den Bosch L, Van Houtte E, Callewaert G, Robberecht W. GluR2-dependent properties of AMPA receptors determine the selective vulnerability of motor neurons to excitotoxicity. J Neurophysiol 2002;88: 1279–87. https://doi.org/10.1152/jn.00163.2002.

[84] von Lewinski F, Keller BU. Ca2+, mitochondria and selective motoneuron vulnerability: implications for ALS. Trends Neurosci 2005;28:494–500. https://doi.org/10.1016/j.tins.2005.07.001.

[85] Lladó J, Tolosa L, Olmos G. Cellular and molecular mechanisms involved in the neuroprotective effects of VEGF on motoneurons. Front Cell Neurosci 2013;7:181. https://doi.org/10.3389/fncel.2013.00181.

[86] Van Damme P, Braeken D, Callewaert G, Robberecht W, Van Den Bosch L. GluR2 deficiency accelerates motor neuron degeneration in a mouse model of amyotrophic lateral sclerosis. J Neuropathol Exp Neurol 2005;64:605–12. https://doi.org/10.1097/01.jnen.0000171647.09589.07.

[87] Ruiz de Almodovar C, Lambrechts D, Mazzone M, Carmeliet P, Almodovar CRDE, Lambrechts D, et al. Role and therapeutic potential of VEGF in the nervous system. Physiol Rev 2009;89:607–48. https://doi.org/10.1152/physrev.00031.2008.

[88] Li B, Xu W, Luo C, Gozal D, Liu R. VEGF-induced activation of the PI3-K/Akt pathway reduces mutant SOD1-mediated motor neuron cell death. Mol Brain Res 2003;111:155–64. https://doi.org/10.1016/S0169-328X(03)00025-1.

[89] Tolosa L, Mir M, Olmos G, Lladó J. Vascular endothelial growth factor protects motoneurons from serum deprivation-induced cell death through phosphatidylinositol 3-kinase-mediated p38 mitogen-activated protein kinase inhibition. Neuroscience 2009;158:1348–55. https://doi.org/10.1016/j.neuroscience.2008.10.060.

[90] Tovar-y-Romo LB, Tapia R. VEGF protects spinal motor neurons against chronic excitotoxic degeneration in vivo by activation of PI3-K pathway and inhibition of p38MAPK. J Neurochem 2010;115:1090–101. https://doi.org/10.1111/j.1471-4159.2010.06766.x.

[91] Wang Y, Duan W, Wang W, Wen Di, Liu Y, Liu Y, et al. scAAV9-VEGF prolongs the survival of transgenic ALS mice by promoting activation of M2 microglia and the PI3K/Akt pathway. Brain Res 2016;1648:1–10. https://doi.org/10.1016/j.brainres.2016.06.043.

[92] Van Damme P, Tilkin P, Mercer KJ, Terryn J, D'Hondt A, Herne N, et al. Intracerebroventricular delivery of vascular endothelial growth factor in patients with amyotrophic lateral sclerosis, a phase i study. Brain Commun 2020;2:1–10. https://doi.org/10.1093/braincomms/fcaa160.

[93] Sumi H, Kato S, Mochimaru Y, Fujimura H, Etoh M, Sakoda S. Nuclear TAR DNA binding protein 43 expression in spinal cord neurons correlates with the clinical course in amyotrophic lateral sclerosis. J Neuropathol Exp Neurol 2009;68:37–47. https://doi.org/10.1097/NEN.0b013e3181919cb5.

[94] Brettschneider J, Arai K, Del Tredici K, Toledo JB, Robinson JL, Lee EB, et al. TDP-43 pathology and neuronal loss in amyotrophic lateral sclerosis spinal cord. Acta Neuropathol 2014;128:423–37. https://doi.org/10.1007/s00401-014-1299-6.

[95] Mizuno Y, Fujita Y, Takatama M, Okamoto K. Comparison of phosphorylated TDP-43-positive inclusions in oculomotor neurons in patients with non-ALS and ALS disorders. J Neurol Sci 2012;315:20–5. https://doi.org/10.1016/j.jns.2011.12.012.

[96] Foulds PG, Davidson Y, Mishra M, Hobson DJ, Humphreys KM, Taylor M, et al. Plasma phosphorylated-TDP-43 protein levels correlate with brain pathology in frontotemporal lobar degeneration. Acta Neuropathol 2009;118:647–58. https://doi.org/10.1007/s00401-009-0594-0.

[97] Tremblay C, St-Amour I, Schneider J, Bennett DA, Calon F. Accumulation of transactive response DNA binding protein 43 in mild cognitive impairment and Alzheimer disease. J Neuropathol Exp Neurol 2011;70:788–98. https://doi.org/10.1097/NEN.0b013e31822c62cf.

[98] Kasai T, Tokuda T, Ishigami N, Sasayama H, Foulds P, Mitchell DJ, et al. Increased TDP-43 protein in cerebrospinal fluid of patients with amyotrophic lateral sclerosis. Acta Neuropathol 2009;117:55–62. https://doi.org/10.1007/s00401-008-0456-1.

[99] Noto Y-I, Shibuya K, Sato Y, Kanai K, Misawa S, Sawai S, et al. Elevated CSF TDP-43 levels in amyotrophic lateral sclerosis: specificity, sensitivity, and a possible prognostic value. Amyotroph Lateral Scler 2011;12:140–3. https://doi.org/10.3109/17482968.2010.541263.

[100] Brettschneider J, Del Tredici K, Toledo JB, Robinson JL, Irwin DJ, Grossman M, et al. Stages of pTDP-43 pathology in amyotrophic lateral sclerosis. Ann Neurol 2013;74:20–38. https://doi.org/10.1002/ana.23937.

[101] Tan C-FF, Eguchi H, Tagawa A, Onodera O, Iwasaki T, Tsujino A, et al. TDP-43 immunoreactivity in neuronal inclusions in familial amyotrophic lateral sclerosis with or without SOD1 gene mutation. Acta Neuropathol 2007;113:535–42. https://doi.org/10.1007/s00401-007-0206-9.

[102] Cai M, Lee K-W, Choi S-M, Yang EJ. TDP-43 modification in the hSOD1(G93A) amyotrophic lateral sclerosis mouse model. Neurol Res 2015;37:253–62. https://doi.org/10.1179/1743132814Y.0000000443.

[103] Marino M, Papa S, Crippa V, Nardo G, Peviani M, Cheroni C, et al. Differences in protein quality control correlate with phenotype variability in 2 mouse models of familial amyotrophic lateral sclerosis. Neurobiol Aging 2015;36:492–504. https://doi.org/10.1016/j.neurobiolaging.2014.06.026.